Acta Technica *62* (2017), No. 7A, 1435–1444

Reconstruction of aircraft shape and surface based on raster projection point cloud

Wei Hou[1]

Abstract. A high order smoothing algorithm based on Laplacian regularization is proposed to solve the problem of surface reconstruction of scattered point cloud data obtained by 3D scanning or 3D reconstruction. Firstly, the bounding box of the point cloud data is calculated and the discrete voxel space is got; secondly, in the voxel space and based on implicit surface gradient and point cloud position, and normal information, objective function is established to control the fairing effect of the reconstructed surface after Laplacian regularization of the objective function; thirdly, according to the principle of optimality, the reconstruction problem is converted to a sparse linear equation solving problem; finally, the triangular mesh representation of the reconstructed surface is obtained by the marching cube algorithm. The experimental results of qualitative and quantitative results show that this method is better than the common Poisson method in terms of the reconstruction surface drawing effect and accuracy.

Key words. Scattered point cloud, 3D scanning, Surface reconstruction, Implicit surface, Marching cube

.

1. Introduction

With the development of optical scanning equipment and the improvement of the performance of multi-view stereo vision algorithm, it is becoming increasingly convenient to obtain the scattered point cloud data reflecting the surface of the object. However, the point cloud data only contains the discrete spatial location information of the surface of the object, and the data size is huge, and it can not be used directly in the actual application [1]. Therefore, the reconstruction of triangular mesh model for the object surface from these unorganized point cloud data is a research focus in recent years [2]. The method of surface reconstruction for scattered point clouds is divided into two main categories, namely, the method based

[1]College of Aerocraft, Xi'an Aeronautical University, Xi'an, Shaanxi, 710077

on computation geometry and the method based on the implicit surface. The idea of computation geometry method is to directly carry out Delaunay triangulation of the point cloud according to the Voronoi diagram [3]. The representative algorithms are Tight Cocone [4] and Power Crust [5]. The disadvantage of this method is that it is sensitive to noise, and it is difficult to obtain a closed reconstruction surface, and the amount of calculation is large. The idea of implicit surface reconstruction is to use an implicit function to fit the point cloud, and take the zero level set of the function as an approximation estimate of the real surface of the object. This method can not only accurately approximate the surface of complex objects at a low computational cost, but also facilitate editing of reconstructed surfaces. Therefore, it has become the most widely used method at present. The implicit surface reconstruction method can be divided into the global method and the local method. The representative methods of global implicit surface reconstruction include surface reconstruction based on Radial Base Function (RBF) [6-8], surface reconstruction based on Poisson equation [9], wavelet based method [10], finite element method and so on. The existing problem of implicit surface reconstruction is how to obtain the fairing surface reconstruction under the premise of keeping the detail features. Inspired by the high order smooth surface extraction algorithm proposed by Victor et al., this paper proposes a high order smooth implicit surface reconstruction method, which preserves the detail features and obtains the fairing reconstruction surface.

2. Algorithmic description

The calculation process of the algorithm in this paper is shown in Fig. 1. First of all, according to the spatial scattered point cloud data, the bounding box is calculated; secondly, the bounding box space is discretized; thirdly, the objective function proposed in this paper is discretized in the voxel space and a set of linear equations is obtained; fourthly, by solving the equations, the implicit surface representation of point cloud is obtained; finally, the marching cube algorithm is used for surface triangular mesh extraction.

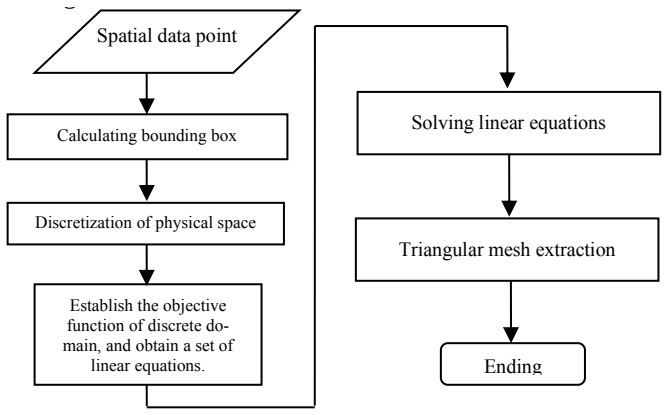

Fig. 1. Algorithm calculation process

3. Objective function

The directed point cloud data are expressed as $\mathbf{D} = \{(\mathbf{p}i,\mathbf{n}i)\}i \in[1,N]$, where $\mathbf{p}i \in\mathbf{R}3$ and $\mathbf{n}i \in\mathbf{R}3$ are respectively the spatial position and normal vector of the *Ith* point. The purpose of implicit surface reconstruction is to estimate the surface $\mathbf{S}$ represented by $\mathbf{D}$ with an implicit equation $f(\mathbf{p}) = 0$, where $f(\mathbf{p}) = \sum wi\Phi i(\mathbf{p})$, wi is the weight coefficient, and $\Phi i(\mathbf{p})$ is the basis function.

In order to estimate $\mathbf{S}$ with $f(\mathbf{p}) = 0$, this article assumes that $\mathbf{D}$ is the sampling point on the surface, which means:

$$f(\mathbf{p}_i) = 0\,. \tag{1}$$

$$\nabla f(\mathbf{p}_i) = \mathbf{n}_i\,. \tag{2}$$

The above two formulas only indicate the condition that the surface of the point cloud shall satisfy. In order to get the smooth reconstruction results, it is necessary to restrict the surface deviating from the point cloud. Inspired by the literature [19], this paper considers the following Laplacian regularization:

$$\int (\Delta f)^2 dV \to \min\,. \tag{3}$$

With a comprehensive consideration of the formulas (1) $\sim$ (3), the following objective function is proposed in this paper for solving implicit surface $f(\mathbf{p})$:

$$\varphi(f) = k_1\varphi_{\mathrm{D}}(f) + k_2\varphi_{\mathrm{S}}(f)\,. \tag{4}$$

Where $\varphi\mathrm{D}(f)$ represents data items, and $\varphi\mathrm{S}(f)$ is a regularized smooth term, and their definitions are shown as formulas (5) and (6) respectively.

$$\varphi_D(f) = \frac{1}{N}\sum_{i=1}^{N}\left[f^2(\mathbf{p}_i) + \|\nabla f(\mathbf{p}_i) - \mathbf{n}_i\|^2\right]. \tag{5}$$

$$\varphi_S(f) = \frac{1}{\int_v dV}\int_V (\Delta f)^2 dV\,. \tag{6}$$

The implicit surface representation of the point cloud can be obtained by minimizing formula (4).

4. Objective function on the discrete domain

A bounding box is calculated by the point cloud data and the bounding box is discretized. Assuming that the number of the voxel in x, y, z direction are set as L, the 3D space elements formed by the voxels obtained is represented by $\boldsymbol{G} = \{1,2,\ldots,L\}\times\{1,2,\ldots,L\}\times\{1,2,\ldots,L\}$. The expression of one individual voxel is as

shown in Fig. 2.

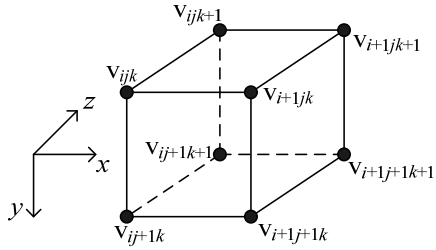

Fig. 2. Voxel representation of discrete physical space

If point $\mathbf{p}$ is a voxel as shown in Fig. 2, then it is obtained after the tri-linear interpolation of the implicit function values at 8 vertices of $f(\mathbf{p})$.

$$\begin{aligned} f(\mathbf{p}) = {} & a_{ijk}f_{ijk} + a_{ijk+1}f_{ijk+1} + a_{ij+1k}f_{ij+1k} + \\ & a_{ij+1k+1}f_{ij+1k+1} + a_{i+1jk}f_{i+1jk} + a_{i+1jk+1}f_{i+1jk+1} + \\ & a_{i+1j+1k}f_{i+1j+1k} + a_{i+1j+1k+1}f_{i+1j+1k+1}\,. \end{aligned} \tag{7}$$

Where, *aijk* represents the tri-linear coordinates of $f(\mathbf{p})$at the vertex V*ijk*, and *fijk* represents the implicit function value at the vertex V*ijk*.

Assuming that the side length of the voxel is h, the gradient of the implicit surface $f(\mathbf{p})$ is estimated using finite difference as follows:

$$\nabla f(\mathbf{p}) \approx \frac{1}{4h}\cdot \begin{pmatrix} f_{i+1jk} - f_{ijk} + f_{i+1jk+1} - f_{ijk+1} + f_{i+1j+1k} - f_{ij+1k} + f_{i+1j+1k+1} - f_{ij+1k+1} \\ f_{ij+1k} - f_{ijk} + f_{ij+1k+1} - f_{ijk+1} + f_{i+1j+1k} - f_{i+1jk} + f_{i+1j+1k+1} - f_{i+1jk+1} \\ f_{ijk+1} - f_{ijk} + f_{ij+1k+1} - f_{ij+1k} + f_{i+1jk+1} - f_{i+1jk} + f_{i+1j+1k+1} - f_{i+1j+1k} \end{pmatrix}. \tag{8}$$

The finite difference estimation of $(\Delta f(\mathbf{p}))2$ is as follows:

$$\begin{aligned} (\Delta f(\mathbf{p}))^2 \approx & \frac{1}{h^4}[(f_{i+1jk} + f_{i-1jk} - 2f_{ijk}) + (f_{ij+1k} + f_{ij-1k} - 2f_{ijk}) \\ & + (f_{ijk+1} + f_{ijk-1} - 2f_{ijk})]^2\,. \end{aligned} \tag{9}$$

Substitute (7) $\sim$ (9) into formula (4) and represent it with matrix, then:

$$\varphi(f) = \mathbf{F}^{\mathrm{T}}\mathbf{Q}\mathbf{F} - 2\mathbf{b}^{\mathrm{T}}\mathbf{F} + c\,. \tag{10}$$

Where, $\mathbf{F}$ represents the column vector formed by the function value of implicit function at the voxel vertex, $\mathbf{Q}$ is obtained by the finite difference separation of $\frac{1}{N}\sum\limits_{i=1}^{N}\left[f^2(p_i) + \|\nabla f(p_i)\|^2\right] + \frac{1}{\sum_{ijk} h^3}\sum\limits_{ijk}(\Delta f)^2$and the column vector $\mathbf{b}$ is obtained by the finite difference separation and discretization of $\sum n_i \nabla f(p_i)$. c has no contri-

bution to the solution of f, and it is not considered here. Use the formula (10) to derive $\mathbf{F}$ and set it as 0, then:

$$\mathbf{Q}^{\mathrm{T}}\mathbf{F} + \mathbf{Q}\mathbf{F} - 2\mathbf{b} = 0\,. \tag{11}$$

Set $\mathbf{A} = (\mathbf{Q}\mathrm{T}+\mathbf{Q})/2$, the formula (11) can be expressed as:

$$\mathbf{A}\mathbf{F} = \mathbf{b}\,. \tag{12}$$

Through the solving of the Formula (12), the implicit surface representation of the point cloud can be obtained.

4.1. Experiment and analysis

In this paper, the algorithm is implemented by C++, the preprocessed conjugate gradient algorithm is used to solve the formula (12), and the triangular mesh is extracted by the marching cube algorithm. The hardware configuration of the experiment is Intel Core2 Duo 2.20 GHz CPU, 2 GB memory; the software configuration is Windows7+Visual Studio 2008. The point cloud data used in the experiment comes from the literature [20], as shown in Fig. 3, in which the ratio of sampling density at the left and right side of Venus is 400:1. The method proposed in this paper is compared with the Poisson surface reconstruction (Poisson) [9], the smooth subdivision implicit surface reconstruction (SPU) [16] and the D4 wavelet method [10].

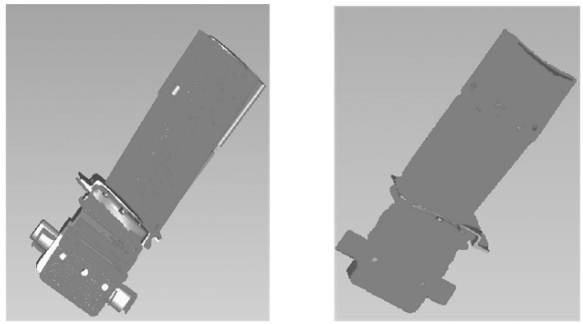

(a) Angel (b) Zoe

Fig. 3. Test point cloud data

4.2. Comparison of computing time and memory consumption

The time for surface reconstruction and the peak memory consumption for cloud data at different points are shown in Tab. 1. The voxel spatial resolution in experiment is 256×256×256. Tab. 2 is the comparison of computing time and memory consumption for different algorithms of Angel point cloud data. Octree structure is used in the Poisson, SPU and D4 wavelets, the depth of which is set as 8 in the

experiment. It can be seen from the table that the calculating time of this method is equivalent to that of Poisson method, and the memory consumption is lower than that of D4 wavelet, but higher than that of Poisson method. This is because this method is the same as the Poisson method, which is to solve a set of sparse linear equations. Unlike Poisson method, octree structure is adopted, so memory consumption is relatively low.

Table 1. Surface reconstruction time of different point clouds

Point cloud name	Point number	Triangular face number of reconstructed surface	Peak memory (MB)	Reconstruction time (s)
Angel	31940	80419	31	35
Zoe	27883	74091	30	35
Venus	72545	67430	32	36

Table 2. Comparison of computing time and memory consumption of different algorithms

Algorithm name	Triangular face number of reconstructed surface	Peak memory (MB)	Reconstruction time (s)
Poisson	66764	17	32
SPU	73880	25	19
D4 wavelet	323912	58	67
This method	80419	31	35

4.3. Comparison of rendering effect of reconstruction surface

Figures 4 to 5 show the rendering effect of different algorithms for the reconstruction of the surface. As shown in Fig. 4, for Angel point cloud data, the Poisson and SPU methods are too smooth to reconstruct the surface, and the details of the mouth and hands are blurred. D4 wavelet and this method keep the better details of reconstructed surface, but the fairing effect of D4 wavelet reconstruction is poor. As shown in Fig. 4, only this method achieves complete reconstruction of the lotus leaf (the dotted frame in the figure) while there are holes in other methods. Similarly, the D4 wavelet and this method keep the better details. The fairing effect of this method is consistent with that of Poisson and SPU, but the fairing effect of D4 wavelet reconstruction surface is poor. As shown in Fig. 5, D4 wavelet reconstruction fails for non-uniform sampling. Seen from the arae as shown in the dotted frame in Fig. 5, the reconstruction results on the right side of the Poisson appear over-smooth phenomenon, and the left transition is not natural; SPU surface reconstruction details are almost smoothed out, and the details of the hair can not be seen; only this method preserves the detail features and achieves smooth reconstruction results.

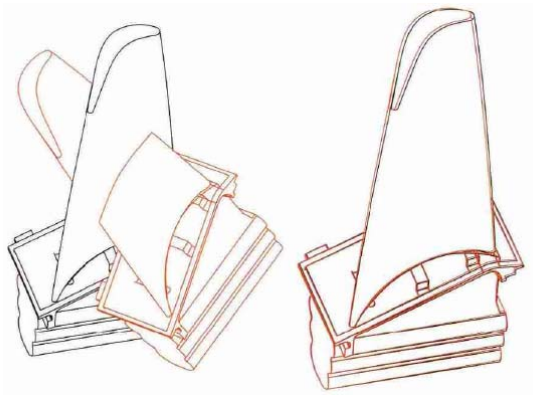

(a) Poisson (d) This method

Fig. 4. Zoe reconstruction results

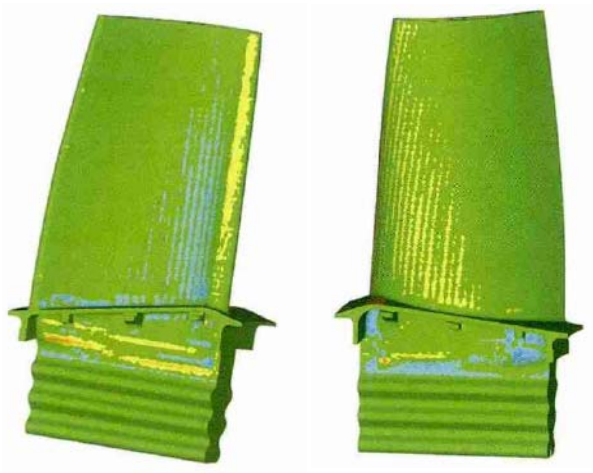

(a) Poisson (d) Method in this paper

Fig. 5. Venus reconstruction results

4.4. Accuracy comparison

According to literature [10], points sampling can be carried out on the known surfaces, and the points sampled can be used to reconstruct the surface and compute the Hausdorff distance between the reconstructed surface and the original surface [21] to judge the accuracy of the algorithm. The smaller the Hausdorff distance is, the higher the accuracy of the reconstruction results will be. In order to make use of the Hausdorff distance for comparison of algorithm accuracy, in this paper, implicit function is used to generate 3 implicit surfaces respectively, namely hollow cube, torus and Jack, as shown in Fig. 6. The spatial points on the implicit surface shown in Fig. 6 are uniformly sampled to form point cloud data, and then Poisson, SPU, D4

wavelet and this method are used for reconstruction. Finally, the Hausdorff distance between the reconstructed surface and the original surface is calculated. Tab. 3 gives the Hausdorff distance of the reconstruction results of different algorithms. The smaller the value is, the closer the reconstruction surface is to the original surface. It can be seen from the table that the accuracy of the SPU reconstruction algorithm is the lowest, and the accuracy of this method is the highest.

Fig. 6. Implicit surface for accuracy comparison

Table 3. Comparison of algorithm accuracy

Point cloud name \ Algorithm name	Poisson	SPU	D4 wavelet	This method
Hollow cube	0.1382	3.1070	0.0786	**0.0605**
Torus	0.0064	1.4597	0.0171	**0.0060**
Jack	0.0929	3.8293	0.0771	**0.0458**

5. Conclusion

In this paper, an objective function is established according to the surface gradient, the location and normal information of point cloud and the Laplacian smoothing regularization. The surface reconstruction problem is converted into a sparse linear equation solving problem by the optimal solution of the function. The experimental results show that this method has high reconstruction accuracy, and the smooth reconstruction results can be obtained while preserving the details. The problem of this method is that the memory consumption is high, only next to that of the D4 wavelet algorithm, next, the octree structure is planned to reduce memory consumption.

Acknowledgement

Shaanxi Natural Science Foundation (2016JQ1043).

References

[1] W. U. Jian-Bo, Q. M. Luo, Y. S. Tan: *Three-dimension surface reconstruction system based on stereo vision and raster projection*[J]. Opto-electronic Engineering *31* (2004), No. 11, 51–54.

[2] Y. Wang, H. Weinacker, B. Koch: *A Lidar Point Cloud Based Procedure for Vertical Canopy Structure Analysis And 3D Single Tree Modelling in Forest*[J]. Sensors *8* (2008), No. 6, 3938–3951.

[3] B. M. J. Haex, S. J. Vander , H. Diers, et al.: *Time-dependent three-dimensional musculo-skeletal modeling based on dynamic surface measurements of bodies: EP*, US7899220[P] (2011).

[4] G. Zheng, L. M. Moskal: *Spatial variability of terrestrial laser scanning based leaf area index*[J]. International Journal of Applied Earth Observation & Geoinformation *19* (2012), No. 1, 226–237.

[5] F. Liu, Q. Z. Teng, Y. U. Yan-Mei, et al.: *An Algorithm for Discriminating Overlapped Stripes in 3D Object Reconstruction Using Phase-Shifting Raster Projection*[J]. Journal of Image & Graphics (2005).

[6] H. Moscovici, A. Verona: *Points clouds generation using TLS and dense-matching techniques.* A test on approachable accuracies of different tools.[J]. *II-5/W1* (2013), No. 12, 1640–1644.

[7] N. Arunkumar, V. Venkataraman, T. Lavanya: *A moving window approximate entropy based neural network for detecting the onset of epileptic seizures.* International Journal of Applied Engineering Research *8* (2013), No. 15, 1841–1847.

[8] J. W. Chan, Y. Y. Zhang, and K. E. Uhrich: *Amphiphilic Macromolecule Self-Assembled Monolayers Suppress Smooth Muscle Cell Proliferation*, Bioconjugate Chemistry *26* (2015) No. 7, 1359–1369.

[9] Y. J. Zhao, L. Wang, H. J. Wang, and C. J. Liu: *Minimum Rate Sampling and Spectrum Blind Reconstruction in Random Equivalent Sampling.* Circuits Systems and Signal Processing *34* (2015), No. 8, 2667–2680.

[10] S. L. Fernandes, V. P. Gurupur, N. R. Sunder, N. Arunkumar, S. Kadry: *A novel nonintrusive decision support approach for heart rate measurement.* Pattern Recognition Letters. https: //doi.org/10.1016/j.patrec.2017.07.002 (2017).

[11] N. Arunkumar, K. Ramkumar, V. Venkatraman, E. Abdulhay, S. L. Fernandes, S. Kadry, S. Segal: *Classification of focal and non focal EEG using entropies.* Pattern Recognition Letters *94* (2017), 112–117.

[12] J. W. Chan, Y. Y. Zhang, and K. E. Uhrich: *Amphiphilic Macromolecule Self-Assembled Monolayers Suppress Smooth Muscle Cell Proliferation*, Bioconjugate Chemistry *26* (2015) No. 7, 1359–1369.

[13] M. P. Malarkodi, N. Arunkumar, N. V. Venkataraman: *Gabor wavelet based approach for face recognition.* International Journal of Applied Engineering Research *8* (2013), No. 15, 1831–1840.

[14] L. R. Stephygraph, N. Arunkumar: *Brain-actuated wireless mobile robot control through an adaptive human-machine interface.* Advances in Intelligent Systems and Computing *397* (2016), 537–549.

Received May 7, 2017